Spontaneous resistive anisotropy in FeZr metallic glasses

1992 J. Phys.: Condens. Matter 4 1993

(http://iopscience.iop.org/0953-8984/4/8/014)

J. Phys.: Condens. Matter 4 (1992) 1993–2008. Printed in the UK

Spontaneous resistive anisotropy in FeZr metallic glasses

H Ma, Z Wang, H P Kunkel and Gwyn Williams
Department of Physics, University of Manitoba, Winnipeg, Manitoba, R3T 2N2, Canada

Received 24 April 1991, in final form 6 August 1991

Abstract. We present measurements of the anisotropy between the longitudinal and transverse magnetoresistance in a number of $Fe_{1-x}Zr_x$ ($0.08 \leqslant x \leqslant 0.11$) metallic glasses in fields ($\mu_0 H_a$) up to 1 T at a number of fixed temperatures between 1.5 and 300 K, and in a single, low field ($\sim$ 5 mT) as a function of temperature. The influence of hydrogen loading was also studied. A low-field (remanent-field) resistive anisotropy (RFRA) first appears at a temperature very close to the Curie temperature (T_C) (found from previous AC susceptibility measurements on the same specimens), confirming the emergence of a substantial, non-local exchange field at this temperature. A linear increase of the RFRA with decreasing temperature immediately below T_C (i.e. as $A(T_C - T)/T_C$) is reported for the first time, and a semiquantitative explanation for such an increase proposed. Structure in the RFRA has also been observed at temperatures well below T_C, although no definite correlation between it and the proposed re-entrant transition in this system could be established.

1. Introduction

The prediction by infinite-range models [1–4] of sequential paramagnetic to ferromagnetic to (transverse) spin-glass transitions in magnetic systems with predominantly ferromagnetic exchange coupling, but which, nevertheless, display significant amounts of exchange bond disorder, has motivated a large number of experimental studies. However, while numerous systems (such as AuFe [5–8], $Eu_xSr_{1-x}S$ [9, 10], NiMn [11, 12] and (PdFe)Mn [13–20]) exhibit experimental features that resemble superficially the behaviour expected to accompany such sequences, detailed quantitative comparisons between experiment and specific model predictions [21] still remain to be carried out. Consequently, it is undecided at present whether experimental characteristics used to designate the lower-temperature ferromagnetic to (transverse) spin-glass phase boundary identify it as a true thermodynamic transition line rather than indicating that it results from the gradual onset of some anisotropy-induced freezing or domain-wall pinning.

In many crystalline systems, the role played by compositional inhomogeneities resulting from metallurgical constraints provides additional complications to understanding the origin of such low-temperature anomalies. In this context the merits of studying amorphous systems—particularly when the alloying element is of low concentration—have recently been emphasized [22]. Among amorphous magnetic systems, FeZr (with > 85 at.% Fe) display many features frequently identified with re-entrant behaviour. It exhibits an obvious transition below room temperature from the paramagnetic state—although the precise character of the transition was initially

0953-8984/92/081993+16$04.50

debated. High-field magnetization studies [23, 24] and small-angle neutron scattering indicated some non-collinearity in the spin structure, whereas recent measurements of the asymptotic critical exponents [25–27] are quite definite in their support of a ferromagnetic transition (these exponent values being close to those predicted by the isotropic three-dimensional Heisenberg model [28]). At still lower temperatures, recent in-field Mössbauer studies [22] have provided strong experimental evidence supporting a subsequent transition into a state with transverse spin-glass ordering (at a temperature designated T_{xy}). Again, however, these Mössbauer data do *not* indicate that this transverse freezing can be classified as critical (rather than gradual), although very recent AC susceptibility measurements [27] revealed that the coefficient ($a_2(T)$) of the leading non-linear contribution to the susceptibility exhibited a distinct, though clearly *not* divergent, anomaly near T_{xy}. While this latter result supports the classification of the behaviour near T_{xy} as critical, it suffers the drawback common to all finite-frequency measurements inherent in such systems: the equilibrium response near the re-entrant boundary is obscured when approached from both above (by the usual hysteretic behaviour associated with a ferromagnetic phase) and below (the low-temperature region is expected to display the constrained critical dynamics found at a direct paramagnetic to spin-glass boundary [29]).

In an attempt to avoid some of these difficulties, and also to complement conventional magnetic response measurements, we have carried out a detailed investigation of the anisotropy of the magnetoresistance in several FeZr metallic glasses in the supposedly re-entrant composition range as a function of field and temperature; the influence of hydrogen loading was also studied. While several studies of the magnetoresistance of the FeZr system have been reported previously (for example, [30]), few measurements of the magnetoresistive anisotropy appear currently available, particularly in the composition range investigated here. The background to such measurements along with the results we have obtained are given below.

2. Experimental details

Magnetoresistance measurements were carried out on amorphous ribbons of Fe_xZr_{1-x} ($x = 0.89$, 0.90, 0.91 and 0.92) produced by melt spinning in a helium atmosphere; complete details of the preparation technique, tests for amorphicity, etc have been given previously [22, 23, 27, 30]. These specimens, of approximate dimensions $32 \times 1 \times 0.02$ mm^3, were mounted in series on a high-thermal-conductivity copper block attached to an insert which could be immersed in a liquid-helium Dewar located between the pole faces of an electromagnet. This electromagnet could be rotated about a vertical axis, enabling measurements to be performed with a field applied parallel ($\parallel$) or perpendicular ($\perp$) to the direction of the sample current (the latter being along the largest specimen dimension); applied fields ($\mu_0 H_a$) of up to 1 T could be produced with the pole-piece separation necessary to accommodate the present experimental arrangement. Four current–voltage contacts were made to each sample using pressure pads, and the differential resistance ratio $[R(H_a,T)-R(0,T)]/R(0,T)$ measured by a low-frequency AC technique [31] using an exciting current of around 10 mA to avoid any self-heating effects; this technique allows the differential resistance ratio to be measured with a resolution of a few parts in 10^5. Measurements were carried out on all samples as a function of applied field H_a at five fixed temperatures (1.6, 4.2, 60, 77 and 295 K; where the temperature

stability is $\leqslant 5$ mK), while the anisotropy $(R_{\parallel} - R_{\perp})/R_0$ was also measured in a single fixed field (the remanent field of the electromagnet, ~ 5 mT) as the samples warmed slowly (~ 1 K min^{-1}) between various refrigerant fixed points (from 60 K to room temperature for all but the 10 at.% Zr specimen, which was subjected to the most detailed measurements, namely between 1.5 and 300 K). Considerable care was taken to ensure that current–voltage contacts were collinear so that no spurious Hall voltage component contributed to the magnetoresistive anisotropy. Temperatures below 4.2 K were achieved by pumping on the He bath, and were found from the bath vapour pressure; above 4.2 K, a Cu coil resistance thermometer or a 100 Ω Allen–Bradly carbon thermometer were used to estimate the specimen temperature.

Hydrogen was introduced into the samples by cathode polarization from a Na_2CO_3 electrolyte and a Pt anode at a constant current density near 10^3 A m^{-2} for a variety of exposure times.

3. The spontaneous resistive anisotropy

The magnetoresistive anisotropy—specifically the spontaneous resistive anisotropy (SRA)—measures the difference in the resistivity of a single-domain ferromagnetic metal in zero induction (B) when the magnetization is aligned parallel or perpendicular to the current direction, via the ratio

$$\Delta\rho/\rho_0 = [\rho_{\parallel}(B) - \rho_{\perp}(B)]_{B\to 0}/\rho_0. \tag{1}$$

While the observation of such an anisotropy was first made over a century ago [32], the SRA remains a relatively little-studied transport coefficient. The interpretation of such data that do exist, whether carried out in terms of an itinerant [33–35] or localized [36–39] model approach, relies on two essential factors: (i) a polarizing field, and (ii) an orbital moment (with spin–orbit coupling) at the scattering site. The polarizing field aligns the spin dipole moment, which then (through spin–orbit coupling) provides a preferred orientation for the orbital contribution with respect to the field (and hence the current). Conduction electrons thus scatter from a slightly different charge cross section depending on the relative orientation of the current and field.

3.1. Localized model

The localized model description of the SRA—which is simpler to understand in principle—is thought to apply, for example, to the case of paramagnetic Ag or Au alloys containing small amounts of rare-earth impurities, which possess well defined total angular momentum J [36–39]. In general, these alloys are not magnetically ordered, so that polarization is induced by applying large external fields. Here, in addition to the usual potential (V) and exchange (Γ_{ex}) scattering terms, an interaction between the conduction electrons (with spin index σ) and the electric quadrupole moment (D) of the 4f electrons can also exist. The scattering potential thus assumes the form [37]:

$$\mathcal{H}_{\text{scat}} = \sum_{k,k'} \left(V + \Gamma_{ex}\sigma \cdot J - \frac{D}{k_F^2}[(J\cdot k)(J\cdot k') - \frac{1}{3}J(J+1)k\cdot k'] \right) a_{k'}^{+} a_k \tag{2}$$

(in the usual notation); while the first two terms are isotropic in polycrystals (exchange scattering can be anisotropic in single crystals [40]), the quadrupole interaction is not, leading to an anisotropy of the form [37–39]

$$[\rho_{\parallel}(B) - \rho_{\perp}(B)]/\rho_0 = (D/V)[\langle J_z^2\rangle - \tfrac{1}{3}J(J+1)] \tag{3}$$

(for $V \gg D$). This anisotropy vanishes in the *paramagnetic* limit as $\langle J_z^2\rangle \to J(J+1)/3$ when $B \to 0$.

3.2. Itinerant model

Itinerant models have been used predominantly to interpret data acquired on ferromagnetic transition-metal host alloys [41] in which polarization is produced by a large exchange field. In these models [33, 34] the magnetic properties of the system are accounted for explicitly by separate consideration of conduction in spin-up (↑) and spin-down (↓) sub-bands. The exchange splitting between these sub-bands results in the properties of electrons near the Fermi energy depending on their spin direction; in particular, the scattering processes themselves can be characterized by a different cross section in each sub-band, with differing associated resistivities, $\rho_\uparrow$ and $\rho_\downarrow$, acting in parallel. The transfer of electrons between sub-bands induced by spin-flip scattering processes (with an associated resistivity $\rho_{\uparrow\downarrow}$ [42]) also contributes to the total resistivity, ρ, which can be expressed as [43]:

$$\rho = [\rho_\uparrow\rho_\downarrow + \rho_{\uparrow\downarrow}(\rho_\uparrow + \rho_\downarrow)]/(\rho_\uparrow + \rho_\downarrow + 4\rho_{\uparrow\downarrow}). \tag{4}$$

The microscopic origin of anisotropy in this model relies on the presence of spin–orbit coupling $\mathcal{H}_{so}$ [44]

$$\mathcal{H}_{so} = \lambda L \cdot S. \tag{5}$$

Basically, the off-diagonal terms $[\lambda/2(L^+S^- + L^-S^+)]$ in this coupling result in an admixture between the two $(2l+1)$-fold orbitally degenerate subgroups, which have been split predominantly by the effect of the exchange field H_{ex} on the spin (with some additional effects arising from the diagonal component of $\mathcal{H}_{so}$). Since this admixture is asymmetric and the orbitally degenerate states display different angular dependences, the scattering of conduction electrons from these states also exhibits an asymmetry relative to the exchange field direction (the magnetization direction). While the underlying physics is thus well understood, calculation of the associated resistive anisotropy is complicated by those same factors that hinder a first-principles calculation of the resistivity, namely a detailed knowledge of the k dependence of the matrix elements of the scattering potential, the introduction of realistic band-structure effects, etc. However, with suitable simplifying assumptions applied to the latter [45], the following expression can be derived for amorphous systems provided γ $(= 3\lambda^2/4H_{ex}^2)$ is small:

$$\Delta\rho/\rho = [\gamma(\rho_{sd\downarrow} - \rho_{sd\uparrow})(\rho_\downarrow - \rho_\uparrow)]/\rho_\uparrow\rho_\downarrow \tag{6}$$

(where $\rho_\uparrow = \rho_{ss\uparrow} + \rho_{sd\uparrow}$, etc, the suffixes being the usual band labels)†

† The well-known result of Campbell *et al* [34]

$$\Delta\rho/\rho = \gamma(\alpha - 1) \qquad \alpha = \rho_\downarrow/\rho_\uparrow$$

which has been applied principally to Ni-based alloys, can be recovered if suitable assumptions are made regarding the dominant contributions to $\rho_\uparrow$ and $\rho_\downarrow$.

Unlike the results derived from a localized model (of crystalline or amorphous systems)—equation (3)—the approach to the paramagnetic limit is not so easily assessed from itinerant model expressions. While it might be argued that, since the numerator vanishes at a ferromagnetic–paramagnetic transition, so that equation (6) yields $\Delta\rho \rightarrow 0$, as is indeed expected, this overlooks the behaviour of γ; the latter, when related simply to exchange-field-induced splittings ($\gamma \propto H_{ex}^{-2}$), exhibits a weak ferromagnetic catastrophe (γ diverges at T_C) [35]. However, the inclusion of an anisotropy/crystal-field-induced splitting K [34] leads to a more general expression for γ ($= 3\lambda^2/4(H_{ex}^2 \pm K^2)$, at least in cubic symmetry), which avoids this catastrophe.

Despite such model difficulties, it has been demonstrated in recent experiments [46, 47] that precision measurements of the longitudinal and transverse magnetoresistance in *low* applied fields can be used as a sensitive probe of an emerging quasi-static exchange field produced by ferromagnetic ordering (*low* applied fields produce no significant changes in either the incipient spin polarization or the trajectories of the current carriers). This technique was then applied to provide the first demonstration of critical behaviour in the SRA through the power-law dependence of the latter on reduced composition ($c/c_0 - 1$) near the ferromagnetic percolation threshold (at $c_0 = 2.25$ at.%) in PdNi.

Here, we attempt to examine the behaviour of the SRA near both transitions in FeZr.

4. Results and discussion

4.1. General features

Figure 1 reproduces the normalized longitudinal and transverse magnetoresistance of the $Fe_{91}Zr_9$ sample at various fixed temperatures as a function of the applied field ($\mu_0 H_a$); the behaviour shown in this figure typifies that shown by the 10 and 11 at.% Zr specimens as well, although the 8 at.% alloy behaves rather differently and consequently is discussed separately. At 295 K the magnetoresistance for both orientations is weakly positive, with $R_\parallel/R_0$ increasing approximately twice as fast as $R_\perp/R_0$. Above 0.2–0.3 T this increase is approximately linear, with $\partial \ln R_\parallel/\partial H_a$ decreasing with increasing Fe concentration from $\sim 8 \times 10^{-4}$ T^{-1} in $Fe_{89}Zr_{11}$ to $\sim 1.5 \times 10^{-4}$ T^{-1} in $Fe_{92}Zr_8$. The overall size of the magnetoresistance is roughly comparable with the Kohler-like contribution observed in Fe-based crystalline alloys [41] scaled for the increase in ρ_0 [48]. There is no evidence for a non-zero SRA either directly in the low-field data or by extrapolation from higher fields. This is expected since the system is paramagnetic ($T_C \simeq 200$ K [22, 23, 27]) and the fields applied are too small to induce any appreciable spin polarization (with an associated negative magnetoresistance, at least in a localized model approach) at this temperature. By contrast, at 77, 58, 4.2 and 1.6 K the presence of a positive SRA is clear, not only by extrapolation from higher-field data, but *directly* via the anisotropy evident near $H_a = 0$ (actually the remanent field of the magnet, some 5–7 mT). Obviously this latter field is of insufficient magnitude to induce any polarization directly at these temperatures; there *must* be a considerable exchange field present (in addition, of course, to spin–orbit coupling). The effect of the small remanent field is simply to modify the domain arrangement so that the magnetization/mean exchange field does *not* average to zero over distances comparable to the conduction-electron mean free

path (in the free-electron approximation the latter is typically about 5 Å in these metallic glasses).

Before discussing further the temperature and composition dependence of the SRA, it is necessary to comment on the procedures used to establish a quantitatively reliable estimate for it. There has been previous discussion [41] on whether the extrapolation from the magnetically saturated regime necessary to determine the SRA from equation (1) should be based on the applied field ($\mu_0 H_a$), the internal field ($\mu_0 H_i$; $H_i = H_a - NM/4\pi$), etc or simply ignored owing to its inherent errors [49]. We have adopted the latter procedure for a number of reasons, the principal one being that, for the FeZr samples studied here, extrapolation from magnetic or technical saturation is not possible since the latter is achieved only in applied fields above 20 T [23], far in excess of those available in the present experiment. The estimates quoted for the SRA and summarized in table 1 are thus based on the simple linear extrapolations using the applied field, as shown in figure 1.

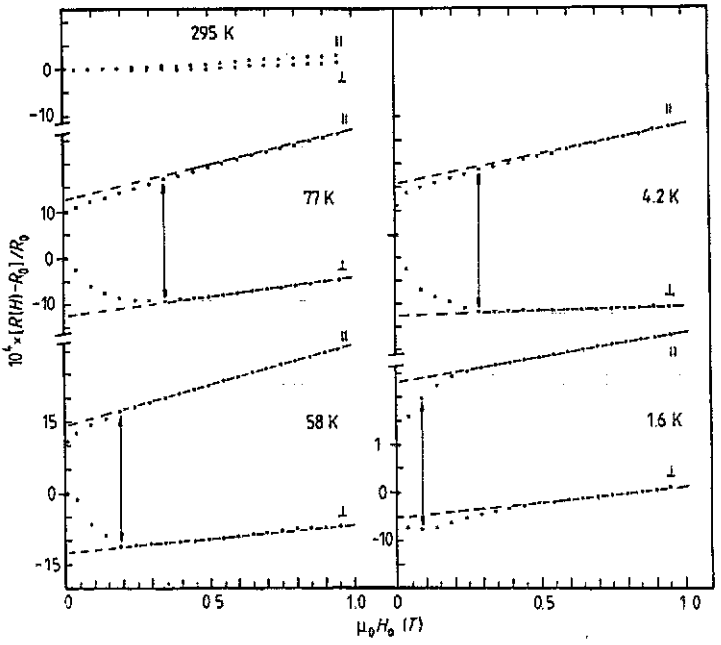

Figure 1. The dimensionless ratio $[R(H)-R_0]/R_0$ (measured for both the longitudinal (||) and transverse (⊥) configurations) plotted against the applied field $\mu_0 H_a$ (in tesla) at various temperatures for the $Fe_{91}Zr_9$ sample. The vertical arrows indicate the anisotropy at H_a^{min}, the field at which the transverse magnetoresistance is a minimum.

As mentioned above, the variations of $R_\parallel/R_0$ and $R_\perp/R_0$ with H_a exhibited by the 9, 10 and 11 at.% Zr samples at all temperatures at and below 77 K are similar, and several features warrant comment. $R_\parallel/R_0$ increases monotonically with H_a; following a rapid low-field variation, this increase is nearly linear between 0.2–0.4 T and the maximum available field (1 T). $R_\perp/R_0$, by contrast, decreases initially, passes through a minimum (at H_a^{min}) and then also displays a near-linear increase at higher field. The result that both $\partial \ln R_\parallel/\partial H_a$ and $\partial \ln R_\perp/\partial H_a$ are positive beyond 0.5 T in these samples is contrary to expectation, as their magnetizations continue to increase substantially with increasing field in this temperature region

Table 1. Estimates of the spontaneous resistive anisotropy (SRA) and of the dimensionless coefficient A (of equation (10)) in the hydrogen-free samples. Entries for both SRA and A should be multiplied by 10^{-4}.

Composition	$T = 77$ K		$T = 58$ K		$T = 4.2$ K		$T = 1.6$ K			
	SRA[a]	SRA[b]	SRA[a]	SRA[b]	SRA[a]	SRA[b]	SRA[a]	SRA[b]	A	T_c(K) [27]
$Fe_{89}Zr_{11}$	31 ± 1	32.5 ± 1	34 ± 1	34.5 ± 1	46.5 ± 1	47.5 ± 1	38 ± 1	38 ± 1	14 ± 1	247
$Fe_{90}Zr_{10}$	30 ± 1	30 ± 1	30.5 ± 1	31 ± 1	42 ± 1	44.5 ± 1	44.5 ± 1	46.5 ± 1	19 ± 1	237
$Fe_{91}Zr_{9}$	24.5 ± 1	25.5 ± 1	26.5 ± 1	28 ± 1	28 ± 1	30 ± 1	28.5 ± 1	28 ± 1	16 ± 1	200
$Fe_{92}Zr_{8}$	24 ± 2	—	25 ± 1	30 ± 1	23 ± 2	—	24 ± 2	—	8 ± 1	182

[a] Using the extrapolation procedure shown in various figures: here the principal source of error arises from uncertainties in the field range over which the 'high-field slope' is attained.

[b] From $\Delta\rho(H_a^{min})$ and equation (8); here we take values of $\Delta\rho(H_a)$ at adjacent field points to H_a^{min} as yielding a representative error.

Table 2. Estimates of the SRA and the coefficient A in the hydrogenated samples; T_C for these samples have not been obtained (from AC susceptibility). Entries for both SRA and A should be multiplied by 10^{-4}.

Composition	$T = 58$ K		$T = 77$ K		$T = 145$ K		$T = 295$ K		
	SRA[a]	SRA[b]	SRA[a]	SRA[b]	SRA[a]	SRA[b]	SRA[a]	SRA[b]	A
$Fe_{89}Zr_{11}+H_2$	Complex	—	—	—	—	—	11 ± 1	12 ± 1	—
$Fe_{90}Zr_{10}+H_2$	41 ± 1	41 ± 1	41.5 ± 1	43 ± 1	26 ± 1	27 ± 1	*Para*	—	23 ± 1
$Fe_{91}Zr_{9}+H_2$	48.5 ± 1	51.5 ± 1	41.5 ± 1	43 ± 1	22 ± 1	22 ± 1	Para	—	—
$Fe_{92}Zr_{8}+H_2$	37 ± 1	37.5 ± 1	35 ± 5	35 ± 1	15.5 ± 1	14.5 ± 1	Para	—	—

[a] By extrapolations.

[b] From $\Delta\rho(H_a^{min})$.

(between 5% and 17% from 0.5 to 20 T at 4.2 K), an effect that frequently produces a negative contribution to the magnetoresistance, at least in a localized spin picture [50]. A possible explanation of this result might be that the non-collinearity in the spin structure (to which the large high-field slope in the magnetization curves has been attributed) occurs on a length scale much larger than the mean free path, so that the magnetization averaged over the latter exhibits a very much weaker field dependence than that displayed by the sample as a whole. In addition, not only are these slopes positive, but their magnitudes are also large (at 77 K, $\partial \ln R_{\parallel}/\partial H_a \sim (12\text{–}15) \times 10^{-4}$ T$^{-1} \simeq 2\partial \ln R_{\perp}/\partial H_a$); some increase in these slopes over those measured in the paramagnetic phase is expected (the applied field, though small, should still induce *some* decrease in localized spin disorder scattering in the paramagnetic state), but the increase observed here is quite marked. At this point it should be recalled that the real quantity of interest—the field-induced magnetoresistivity at constant volume and temperature $\partial \ln \rho/\partial H|_{V,T}$—is related to the quantity actually measured—the logarithmic derivative of the resistance with respect to field (at constant pressure and temperature) $\partial \ln R/\partial H|_{P,T}$, in the isotropic approximation, by [51]:

$$\left(\frac{\partial \ln \rho}{\partial H}\right)_{V,T} = \left(\frac{\partial \ln R}{\partial H}\right)_{P,T} + \left[\frac{1}{3} - \left(\frac{\partial \ln \rho}{\partial \ln V}\right)_T\right]\left(\frac{\partial \ln V}{\partial H}\right)_{P,T}. \quad (7)$$

Recent measurements of the forced volume magnetostriction $\partial \ln V/\partial H|_{P,T}$ in FeZr [52] indicate it to be large compared with other metallic glasses [53], with values in the range $(2\text{–}3.5) \times 10^{-4}$ T^{-1} below room temperature. Despite this, however, with values for $\partial \ln \rho/\partial \ln V$ in the range ± 1, typical of metallic glasses, the measured slopes do not seem to originate from magnetovolume effects. Confirmation for this conclusion comes from data on the $Fe_{89}Zr_{11}$ sample in which the measured forced volume magnetostriction values are comparable at 77 and 293 K [52] whereas the measured slopes $\partial \ln R/\partial H$ are not. The slopes evident in figure 1 at and below 77 K are comparable† with those observed in a number of $Fe_{80-x}Cr_xB_{20}$ metallic glasses [51] (where, at 4.2 K, $\partial \ln R_{\perp}/\partial H_a \sim 3 \times 10^{-4}$ T^{-1}), as is the SRA. By contrast, data on $Fe_{42}Zr_{58}$ [30]—one of the few ferromagnetic FeZr glasses on which magnetoresistive *anisotropy* measurements have been reported—indicate that $\partial \ln R_{\parallel}/\partial H_a \simeq \partial \ln R_{\perp}/\partial H_a \simeq 0.6 \times 10^{-4}$ T^{-1} at 77 K, far below the values observed here, with a correspondingly smaller SRA ($\sim 0.6 \times 10^{-4}$).

Returning to the evaluation of the SRA and the one consistent feature of $R_{\perp}(H_a)$—the appearance of a minimum at H_a^{min}—table 1 also lists values for

$$\Delta R(H_a^{min})/R_0 = [R_{\parallel}(H_a^{min}) - R_{\perp}(H_a^{min})]/R_0. \quad (8)$$

A recent suggestion that this ratio provides an estimate for the SRA consistent with that found by extrapolation methods [47] is confirmed by the data acquired here (in those cases where comparison is possible).

Data obtained from the $Fe_{92}Zr_8$ specimen are shown in figure 2. While $R_{\parallel}/R_0$ again increases monotonically with field, exhibiting a slope $\partial \ln R_{\parallel}/\partial H_a$ beyond

† Nevertheless, they are still over an order of magnitude smaller than those reported for PdNi in the vicinity of the critical composition necessary to establish a ferromagnetic ground state [46, 47]. Since the slopes $\partial \ln R_{\parallel}/\partial H$ increase with increasing Fe concentration above 89 at.%, they may yet provide some indications as to the nature of the conjectured ground state for amorphous Fe [23].

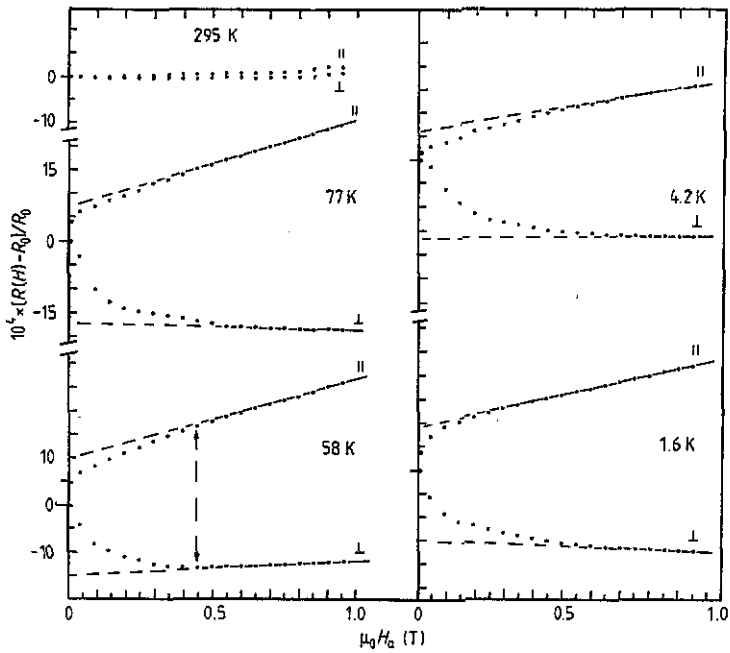

Figure 2. The dimensionless ratio $[R(H) - R_0]/R_0$ for the $Fe_{92}Zr_8$ sample (measured for both the longitudinal (||) and transverse (⊥) configurations) plotted against the applied field $\mu_0 H_a$ (in tesla) at various temperatures. Notice that a minimum in the transverse magnetoresistance $R_\perp(H_a^{min})$ occurs at 58 K alone for this specimen.

0.3 T which is even larger than that found in other specimens at 77 K and below, $\partial \ln R_\perp/\partial H_a$ does not become positive (with the exception of the data around 58 K). Furthermore, $\partial \ln R_\perp/\partial H_a$ does not exhibit an extended linear region at the various fixed temperatures from which an extrapolation to $H_a = 0$ can be made with any confidence; the corresponding SRA estimate based on this extrapolation thus has a larger associated error (table 1). For this sample, estimates for the SRA based on H_i rather than H_a would be larger, a result consistent with the one available estimate for the SRA based on the use of equation (8) and the appearance of a minimum in the transverse magnetoresistance at 58 K alone. That this transverse component is dominated by a negative contribution at other fixed temperatures† below T_C may result from the magnetization in the 8 at.% Zr sample in fields of 1 T being substantially further removed from saturation than that in other samples [23], and its higher coercive field [22].

The dilation exhibited by ferromagnetic metallic glasses is usually isotropic; however, recent measurements on FeZr (with > 88 at.% Fe) have revealed an anisotropy in the longitudinal ($\lambda_\parallel = \delta L/L$ parallel to H_a) and transverse magnetostriction ($\lambda_\perp = \delta L/L$ perpendicular to H_a) below T_C [52]. In particular, in the case of $Fe_{92}Zr_8$ for which detailed measurements have been reported at 4.2 K, the possible contribution from such an anisotropy to the SRA can be examined. The relevant terms, from an appropriate generalization of equation (7), come from the integrated effects of competing contributions from $(\partial \ln \rho/\partial V)(\partial \lambda_\parallel/\partial H)$ and

† The origin of a positive $\partial \ln R_\perp/\partial H$ near 58 K alone is currently unclear; it *may* be linked with the proposed onset of transverse spin freezing just below 77 K reported recently for this sample [22].

$(\partial \ln \rho/\partial V)(\partial \lambda_\perp/\partial H)$. Not only do the signs of these contributions to the SRA appear to be the same, but so are their magnitudes ($\sim 10^{-4}$ T^{-1} for $\partial \ln \rho/\partial \ln V \sim 1$). This result, combined with that deduced previously from equation (7), suggests that magnetovolume effects lead to uncertainties in the SRA comparable with the errors listed in table 1. Consequently, such effects will be neglected in subsequent discussion and the SRA treated as though it were estimated from the magnetoresistivity rather than the normalized magnetoresistance.

The general features of the SRA listed in table 1 are first their magnitude (typically $(3\text{–}4) \times 10^{-3}$), secondly their composition dependence (they increase with decreasing Fe concentration) and thirdly their temperature dependence (they tend to increase with decreasing temperature). These will be discussed below along with the detailed temperature dependence of the remanent-field anisotropy.

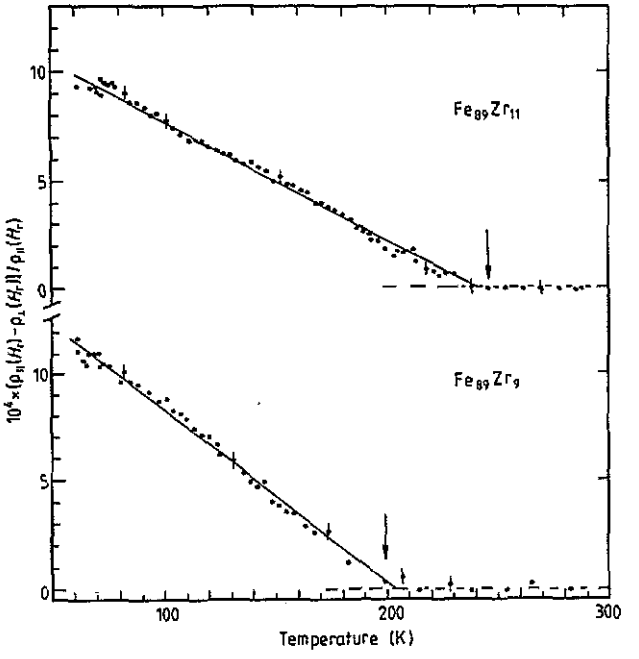

Figure 3. The dimensionless RFRA $[\rho_\parallel(H_r) - \rho_\perp(H_r)]/\rho_\parallel(H_r)$ (measured above 60 K in the remanent field $\mu_0 H_r \sim 5$ mT of the magnet) plotted against temperature (in Kelvin) for two of the samples. The vertical arrows indicate the Curie temperatures of the same specimens found from AC susceptibility measurements.

4.2. Temperature dependence of the remanent-field anisotropy

Figure 3 reproduces the detailed temperature dependence of the resistive anisotropy

$$\Delta\rho(H_r)/\rho_0 = [\rho_\parallel(H_r) - \rho_\perp(H_r)]/\rho_0 \tag{9}$$

measured in the approximately 5 mT remanent field ($\mu_0 H_r$) of the electromagnet, as a function of temperature from 60 K to room temperature, on 9 and 11 at.% Zr samples. In particular, considerable emphasis was placed on attempting to determine the temperature at which this anisotropy first vanished, since, in these low applied

fields ($\mu_0 H_r$), this would indicate the collapse of the exchange field $\mu_0 H_{ex}$ associated with ferromagnetic ordering†. As can be seen from this figure, there is very good agreement between this latter temperature and the Curie temperature T_C determined from AC susceptibility measurements on the same samples [27]; this provides strong support for the occurrence of predominantly ferromagnetic correlations over length scales comparable to the mean free path, if not for long-ranged ferromagnetic ordering, in these samples. It can also be seen from figure 3 (in fact, in all the specimens studied) that this remanent-field resistive anisotropy (RFRA) increases approximately linearly with decreasing temperature below T_C, namely

$$\Delta\rho(H_r)/\rho_0 = A(T_C - T)/T_C \qquad T < T_C \tag{10}$$

over a wide interval ($T \geqslant 60$ K $\simeq T_C/4$), with the coefficient A displaying a marked reduction in the 8 at.% Zr sample (table 1). Such behaviour is consistent with the predictions of a localized model when treated in mean field, provided certain additional constraints are satisfied. According to this model, the temperature dependence of the RFRA—from equation (3)—would vary as

$$\Delta\rho(H_r, T) \propto \langle M_z^2 \rangle \simeq \langle M_z \rangle^2 = [(T_C - T)/T_C]^{2\beta} \tag{11}$$

provided the temperature dependence of

$$\langle M_z^2 \rangle = \langle M_z \rangle^2 + \chi T$$

(from the fluctuation–dissipation theorem) is dominated by the first term (i.e. that the field-dependent susceptibility below T_C is not strongly temperature-dependent [27]) and H_r is not too large; equation (11) reproduces the observed temperature dependence when $\beta = \frac{1}{2}$. It is certainly well established experimentally [54] and theoretically [50] that the low-field magnetoresistance varies as $\langle M_z \rangle^2$; however, no previous report of the low-field resistive *anisotropy* behaving in the above manner has been made. Of course, it is not expected that this temperature dependence holds in the immediate vicinity of T_C where critical fluctuations play a dominant role.

Figure 4 presents similar results from the $Fe_{90}Zr_{10}$ specimen, the only sample in which the remanent-field anisotropy was measured below 60 K. A linear increase of the remanent-field anisotropy with decreasing temperature below a well defined temperature very close to T_C is again evident; however, on cooling below 60 K, structure‡ appears in this anisotropy and the latter exhibits a maximum between 55 and 65 K, and a broad (local) minimum between 6 and 20 K.

While it might be appealing to identify elements in this structure with the onset of the conjectured re-entrant transition, such an identification can currently, at best, be described as tentative. Certainly earlier phase diagrams for this system gave T_{xy} for $Fe_{90}Zr_{10}$ in the range 50–56 K [23], close to the temperature of the maximum in figure 4. However, recent estimates for T_{xy} in $Fe_{92}Zr_8$ and $Fe_{91}Zr_9$ (based on detailed in-field Mössbauer measurements [22] and the behaviour of the leading non-linear term in the AC susceptibility [27]) indicate it to be much reduced compared with these earlier values. Since no such detailed measurements currently exist for

† Actually, an indication of the temperature at which $\langle H_{ex} \rangle_l$—the exchange field averaged over distances of the order of the conduction electron mean free path l—vanishes.

‡ Such structure *may* also be present in the other samples below 60 K.

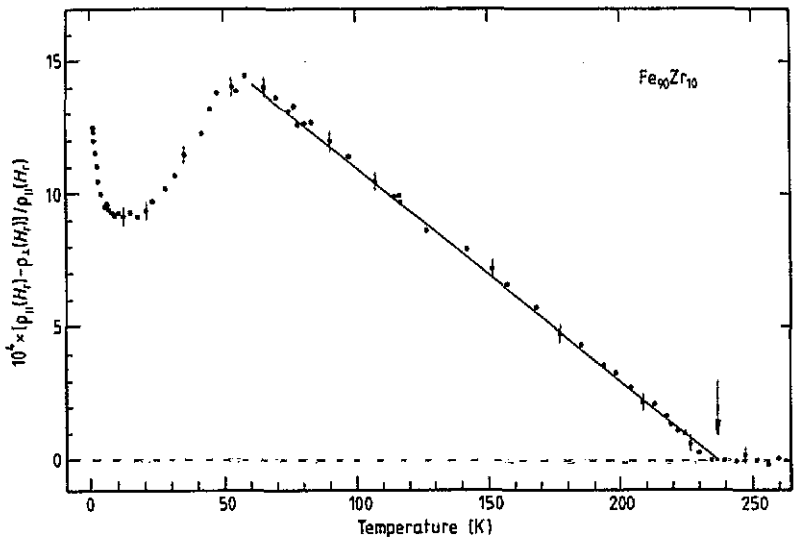

Figure 4. The dimensionless RFRA $[\rho_{\parallel}(H_r) - \rho_{\perp}(H_r)]/\rho_{\parallel}(H_r)$ plotted against temperature (in Kelvin) for the $Fe_{90}Zr_{10}$ specimen. Its Curie temperature (from AC susceptibility measurements) is indicated by the vertical arrow.

$Fe_{90}Zr_{10}$, it is not known whether the revised T_{xy} would be lowered sufficiently to place it in the vicinity of the minimum in the remanent-field anisotropy. Furthermore, it should be made clear that the SRA (determined by extrapolation from 'high' field) *does not exhibit such structure; in* $Fe_{90}Zr_{10}$ *the* SRA (*measured, admittedly, at* only four temperatures below T_C, these being the only fixed temperatures at which complete field sweeps could be obtained) increases monotonically with decreasing temperature (figure 5(*a*)), with the structure visible in the remanent-field anisotropy emanating from changes in the *low*-field magnetoresistance (figure 5(*b*)). Indeed, it would seem that the SRA (specifically, the anisotropy deduced by extrapolation from fields high enough to achieve 'technical' saturation) may *not* be an appropriate parameter to investigate near a direct or re-entrant spin-glass transition, since the use of high fields might influence the freezing of the random spin component. As in susceptibility/ magnetization studies, the judicious use of fields large enough to reveal the relevant effects (namely to establish the leading non-linear term in the magnetization with suitable accuracy) yet small enough not to modify the spin arrangement substantially appears necessary. Whether the ~ 5 mT remanent field used here satisfies these criteria remains an open question. Nevertheless, in view of the very recent report of ultra-low-field (~ 0.2 mT) magnetoresistance measurements on re-entrant systems [55], which tentatively identifies qualitative features in such data with re-entrant behaviour, the publication of the present results seems timely.

To return to the discussion of the general features of the present data in terms of model approaches, in view of the Fe concentration existing in these samples, an itinerant model approach appears appropriate in spite of the agreement between the measured and localized model critical exponents at T_C, and the behaviour reported for the low-field resistive anisotropy as a function of temperature below T_C. The observation of a positive SRA in all the samples examined does not allow the relative magnitudes of $\rho_{sd\downarrow}$ and $\rho_{sd\uparrow}$ to be determined in amorphous systems (through equation (6)) as did the compact expression of Campbell *et al* [34] in the case of

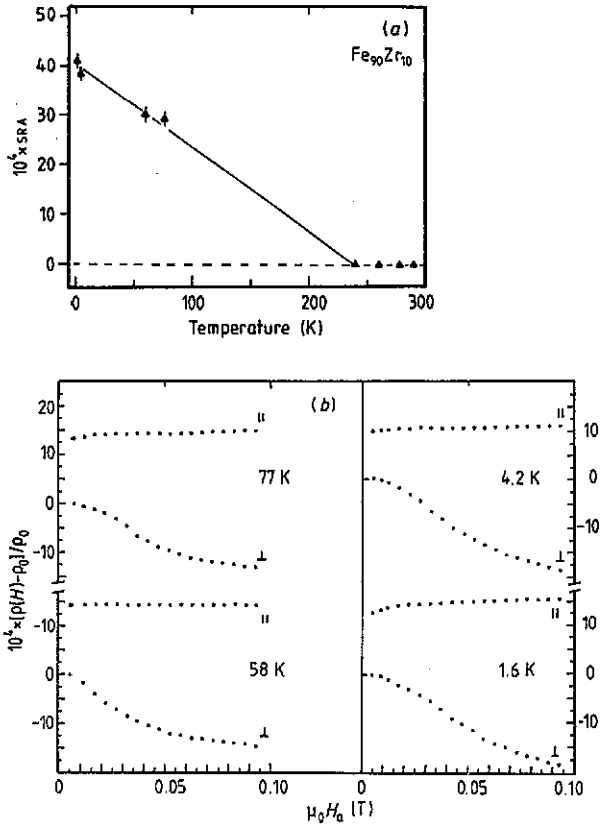

Figure 5. (*a*) The spontaneous resistive anistropy ratio (found from complete field sweeps at four fixed temperatures—as described in the text) plotted against temperature (in Kelvin) for the $Fe_{90}Zr_{10}$ sample. (*b*) Details of the magnetoresistance measured in low applied fields ($\mu_0 H_a \leqslant 0.1$ T) for the $Fe_{90}Zr_{10}$ specimen at a number of temperatures.

strong crystalline ferromagnets (and previously applied to this system [56]). Even assuming $\rho_{ss\uparrow} = \rho_{ss\downarrow}$ in these samples does not remove this ambiguity, as now $\Delta\rho \propto (\rho_{sd\downarrow} - \rho_{sd\uparrow})^2$; with γ taken as 10^{-2} the low-temperature data in table 1 yield

$$(\rho_{sd\downarrow} - \rho_{sd\uparrow})^2/\rho_\downarrow\rho_\uparrow \sim 0.2\text{–}0.4 \tag{12}$$

the magnitude of which suggests weak ferromagnetism. This is confirmed by recent band-structure calculations [57], which, for $Fe_{93}Zr_7$, predict that the density of states at the Fermi energy E_F for either spin orientation is substantial, with that for up spins $N_\uparrow(E_F)$ exceeding $N_\downarrow(E_F)$ by only $\sim 10\%$†.

Several possible explanations for the increase in the SRA with decreasing Fe concentration could be forwarded (based on the increase in T_C, with associated changes in the spin-up and spin-down sub-band occupations induced by a varying exchange

† Taking the resistivity to be proportional to some matrix element squared multiplied by the density of states would suggest $\rho_{sd\uparrow} > \rho_{sd\downarrow}$ if the matrix element is spin-independent. This conclusion conflicts with that drawn earlier [56] using the correspondingly crude approximation in which these samples are treated as strong ferromagnets with a resistivity dominated by s–d scattering.

splitting), but, considering the lack of explicit band-structure calculations for these particular compositions, such discussion would be inconclusive. On the other hand, the observation of a decreasing SRA with increasing temperature can be understood on general grounds. As the temperature is increased, thermal fluctuations compete with the exchange splitting, leading to an equalization in the sub-band occupations; the difference between the two terms in the numerator of equation (12) decreases, as does the SRA. This process evolves continuously (provided no pathological structure exists in the density of states) until the Curie temperature is reached, at which point the static exchange splitting collapses, $\rho_{ss\uparrow} = \rho_{ss\downarrow}, \rho_{sd\uparrow} = \rho_{sd\downarrow}$ and the SRA vanishes (provided, of course, some anisotropy/crystal-field-induced splitting exists [35]). The localized model, however, appears to make a quantitative explanation of this temperature dependence possible.

Having discussed the general features of the SRA and the temperature dependence of the remanent-field anisotropy, we finally turn to a brief discussion of the effects of hydrogen charging.

4.3. Effects of hydrogenation

The data reported below were acquired on samples that had been hydrogenated for some 2 min at $\sim 10^3$ A m^{-2}. (No direct means of establishing the hydrogen concentration is currently available to us, so we simply indicate the charging conditions; comparisons with existing data [58], however, suggest a H/Zr ratio near 1. With only a qualitative measure of the degree of hydrogen loading, a brief summary alone of its effects will be presented.) The introduction of hydrogen into amorphous FeZr is known to increase T_C and, when saturated, raises the Fe moment to around $2\mu_B$ and eliminates the high-field slope in the magnetization curves, so that the samples become soft ferromagnets achieving saturation in fields of approximately 0.1 T [23]. Furthermore, since the presence of hydrogen eliminates the spin-glass transition [58], these measurements concentrated on the temperature region above 58 K (as a result of the latter, slight modifications to the apparatus were made that enabled complete field sweeps to be carried out near 145 K also).

The changes induced by the present hydrogen loading process were that it basically eliminates the previously described differences between the 8 at.% Zr sample and the other specimens, while complicating the properties of the 11 at.% sample. Specifically, data on the hydrogenated $Fe_{92}Zr_8$, $Fe_{91}Zr_9$ and $Fe_{90}Zr_{10}$ samples indicated that they remain paramagnetic at room temperature, although their magnetoresistance increases by typically a factor of 2 at that temperature compared with the hydrogen-free condition (see table 2).

In the hydrogenated $Fe_{89}Zr_{11}$ specimen, the elevation of T_C with hydrogen loading is clearly evident as a positive SRA (estimated by extrapolation and through equation (8)) is apparent at room temperature. On cooling, however, considerable modifications occur in both the longitudinal and transverse magnetoresistance, which makes quantitative analysis difficult.

Increasing the hydrogen loading further results in similar complicating features appearing progressively in the other specimens; such data will not be presented at this time.

Returning to table 2, the general features of the SRA summarized there are that these anisotropies behave similarly with temperature and composition to the unhydrogenated samples, although the magnitudes for the SRA are enhanced overall. Having

discussed this temperature and composition dependence in section 4.2, it simply remains to comment on the increased magnitude of the SRA following hydrogenation. The influence of the latter on the mean Fe moment has been investigated through band-structure studies [59], which conclude that this moment is increased as a result of a transfer of electrons from the spin-down to the spin-up sub-band (induced by the underlying volume expansion accompanying hydrogen loading). As this transfer occurs, the Fermi level is relocated, and in the case of $Fe_{93}Zr_7H_{14}$ this results in $N_\uparrow(E_F)$ becoming considerably larger than $N_\downarrow(E_F)$. The admittedly crude approximation of replacing $\rho_{sd\uparrow}$ and $\rho_{sd\downarrow}$ in equation (12) by $N_\uparrow(E_F)$ and $N_\downarrow(E_F)$ nevertheless yields a large increase in the SRA, in general agreement with the experimental observations.

The temperature dependence of the RFRA in the hydrogenated $Fe_{90}Zr_{10}$ sample has also been measured above 60 K. It exhibits a similar behaviour to that seen in the hydrogen-free samples, although the coefficient A is enhanced and the anisotropy now vanishes near 260 K, confirming the elevation of T_C in this sample.

5. Conclusions and summary

Measurements of the resistive anisotropy in a series of amorphous $Fe_{1-x}Zr_x$ ($0.08 \leqslant x \leqslant 0.11$) metallic glasses as a function of temperature, field and hydrogen loading have been carried out. A spontaneous resistive anisotropy first appears at a temperature very close to the ferromagnetic ordering temperature, deduced from previous magnetic studies, in all samples examined; this confirms the emergence of an exchange field at that temperature. A linear increase in the low-field resistive anisotropy with decreasing temperature below T_C has been observed for the first time, and a semiquantitative explanation for this effect has been suggested. Structure in the temperature dependence of the low-field resistive anisotropy in the 10 at.% Zr specimen well below T_C has also been observed, but no definite connection between such structure and the onset of the conjectured re-entrant transition in this system could be established.

Acknowledgments

We would like to thank Professors J O Ström-Olsen and D H Ryan of McGill University for providing the FeZr samples used in this study, and the Natural Sciences and Engineering Research Council (NSERC) of Canada and the Research Board of the University of Manitoba for support.

References

[1] Sherrington D and Kirkpatrick S 1975 *Phys. Rev. Lett.* **35** 1792
Cragg D M, Sherrington D and Gabay M 1982 *Phys. Rev. Lett.* **49** 158
[2] Southern B W 1976 *J. Phys. C: Solid State Phys.* **9** 4011
[3] Gabay M and Toulouse G 1981 *Phys. Rev. Lett.* **47** 201
[4] Binder K and Young A P 1986 *Rev. Mod. Phys.* **58** 801
[5] Coles B R, Sarkissian B V B and Taylor R H 1978 *Phil. Mag.* **37** 489
[6] Lauer J and Keune K 1982 *Phys. Rev. Lett.* **48** 1850

[7] Murani A 1983 *Phys. Rev.* B **28** 432
[8] Campbell I A 1986 *Hyperfine Interact.* **27** 15
[9] Shapiro S 1988 *Spin Waves and Magnetic Excitations* vol 2, ed A S Borovik-Romanov and S K Sinha (Amsterdam: Elsevier) ch 5
[10] Maletta H and Felsch W 1980 *Z. Phys.* B **37** 55
[11] Abdul-Razzaq W and Kouvel J S 1987 *Phys. Rev.* B **35** 1764
[12] Mirebeau I, Itoh S, Mitsuda S, Watanabe T, Endoh Y, Hennion M and Papoular R 1990 *Phys. Rev.* B **41** 11405
[13] Verbeek B H, Nieuwenhuys G J, Stocker H and Mydosh J A 1978 *Phys. Rev. Lett.* **40** 586
[14] Sato T and Miyako Y 1982 *J. Phys. Soc. Japan* **51** 1394
[15] Sato T, Nishioka T, Miyako Y, Takeda Y, Morimoto S and Ito A 1985 *J. Phys. Soc. Japan* **54** 1989
[16] Takeda Y, Morimoto S, Ito A, Sato T and Miyako Y 1985 *J. Phys. Soc. Japan* **54** 2000
[17] Kettschau A, Boysen B, Brewer W D and Campbell I A 1983 *J. Magn. Magn. Mater.* **37** L1
[18] Shapiro S, Shirane G, Verbeek B H, Nieuwenhuys G J and Mydosh J A 1980 *Solid State Commun.* **36** 167
[19] Gist G A, Dodds S A, MacLaughlin D E, Cooke D W, Heffner R H, Hutson R L, Schillaci M E, Boekema C, Mydosh J A and Nieuwenhuys G J 1986 *Phys. Rev.* B **34** 1683
[20] Kunkel H P and Williams G 1988 *J. Magn. Magn. Mater.* **75** 98
[21] Kornik K, Roshko R M and Williams G 1989 *J. Magn. Magn. Mater.* **81** 323
[22] Ryan D H, Ström-Olsen J O, Provencher R and Townsend M 1988 *J. Appl. Phys.* **64** 5787
[23] Ryan D H, Coey J M D, Batalla E, Altounian Z and Ström-Olsen J O 1987 *Phys. Rev.* B **35** 8360
[24] Rhyne J J, Erwin R W, Fernandez-Baca J A and Fish G E 1988 *J. Appl. Phys.* **63** 4080
[25] Kaul S 1987 *J. Appl. Phys.* **61** 451
[26] Kaul S 1988 *J. Phys. F: Met. Phys.* **18** 2089
[27] Ma H, Kunkel H P and Williams G 1991 *J. Phys.: Condens. Matter* **3** 5563
[28] LeGuillou L C and Zinn-Justin J 1980 *Phys. Rev.* B **21** 3976
[29] Geschwind S, Huse D A and Devlin G E 1990 *Phys. Rev.* B **41** 4854
[30] Trudeau M L and Cochrane R W 1991 *Phys. Rev.* B **41** 10535
[31] Muir W B and Ström-Olsen J O 1976 *J. Phys. E: Sci. Instrum.* **9** 163
[32] Thomson W 1857 *Proc. R. Soc.* **8** 546
[33] Mott N F 1936 *Proc. R. Soc.* A **153** 699
[34] Campbell I A, Fert A and Jaoul O 1970 *J. Phys. C: Solid State Phys.* **3** 595
[35] Malozemoff A P 1986 *Phys. Rev.* B **34** 1853
[36] Kondo J 1962 *Prog. Theor. Phys. (Kyoto)* **27** 772
[37] Friederich A and Fert A 1974 *Phys. Rev. Lett.* **33** 1214
[38] Fert A, Asomoza R, Sanchez D H, Spanjaard D and Friederich A 1977 *Phys. Rev.* B **16** 5040
[39] Fert A and Levy P M 1977 *Phys. Rev.* B **16** 5052
[40] Press M J and Hedgcock F T 1969 *Phys. Rev. Lett.* **23** 167
[41] Dorleijn J W F 1976 *Philips Res. Rep.* **31** 287
[42] Fert A 1969 *J. Phys. C: Solid State Phys.* **2** 1784
[43] Fert A and Campbell I A 1968 *Phys. Rev. Lett.* **21** 1190
[44] Smit J 1951 *Physica* **17** 612
[45] Malozemoff A P 1985 *Phys. Rev.* B **32** 6080
[46] Kunkel H P, Wang Z and Williams G 1987 *J. Phys. F: Met. Phys.* **17** L157
[47] Kunkel H P, Wang Z and Williams G 1989 *J. Phys.: Condens. Matter* **1** 3381
[48] Altounian Z and Ström-Olsen J O 1983 *Phys. Rev.* B **27** 4149
[49] Hsu Y, Jen S and Berger L 1979 *J. Appl. Phys.* **50** 1907
[50] Yosida K 1957 *Phys. Rev.* **107** 396
[51] Olivier M, Ström-Olsen J O and Altounian Z 1987 *Phys. Rev.* B **35** 333
[52] Tange H, Tanaka Y, Goto M and Fukamichi K 1989 *J. Magn. Magn. Mater.* **81** L243
[53] Ishio S and Takahashi M 1985 *J. Magn. Magn. Mater.* **50** 93
[54] Cochrane R W, Hedgcock F T and Ström-Olsen J O 1973 *Phys. Rev.* B **8** 4262
[55] Barnard R D 1990 *J. Phys.: Condens. Matter* **2** 5191
[56] Ma H, Wang Z, Kunkel H P, Williams G and Ryan D H 1990 *J. Appl. Phys.* **67** 5964
[57] Krey U, Krompieski S and Krauss U 1990 *J. Magn. Magn. Mater.* **86** 85
[58] Yu Boliang, Ryan D H, Coey J M D, Altounian Z, Ström-Olsen J O and Razavi F 1983 *J. Phys. F: Met. Phys.* **13** L217
[59] Krompiewski S, Krauss U and Krey U 1989 *Phys. Rev.* B **39** 2819